

This article was presented at the LII Scientific and Educational Conference of ITMO University, January 31 – February 03, 2023, St. Petersburg, Russia

# Sol-Gel Synthesis of Uniform Arrays of Ag and Au Nanoparticles

P.A. Bogdanov<sup>1,\*</sup>, L.A. Sokura<sup>1,2</sup>, A.V. Kremleva<sup>1</sup>, V.V. Vitkin<sup>1</sup>

<sup>1</sup> Institute of Advanced Data Transfer Systems, ITMO University, Kronverkskiy pr. 49, St. Petersburg, 197101, Russia

<sup>2</sup> Ioffe Institute, Politekhnikeskaya str. 26, St. Petersburg, 194021, Russia

---

## Article history

Received March 10, 2023  
Received in revised form  
March 25, 2023  
Accepted March 28, 2023  
Available online March 31, 2023

## Abstract

The obtaining of uniform arrays of silver and gold nanoparticles with a surface density up to  $3.3 \cdot 10^9 \text{ cm}^{-2}$  on the zinc oxide buffer layers by sol-gel method is described. The variations of the solution composition and synthesis mode, layers coating and subsequent heat treatment were carried out. The absorption spectra of the obtained samples had a peak near 400–570 nm corresponding to the plasmon resonance in the Ag and Au nanoparticles. Wavelength and shape of Ag and Au nanoparticles plasmon peak varied depending on the synthesis mode: the use of ZnO buffer layers leads to an increase in the intensity of the nanoparticles plasmon peak, the annealing leads to a gradual decrease and broadening of the absorption peak of Ag and mixed Ag and Au nanoparticles arrays, but does not affect the peak of Au nanoparticles.

---

**Keywords:** SERS; Sol-gel synthesis of nanoparticles; Plasmon absorption peak; Au and Ag nanoparticles; Scanning electron microscopy

## 1. INTRODUCTION

Many fields of science, such as medicine [1,2] and criminalistics [3,4], require the ability to detect substances from their small amount. One of these techniques is a surface-enhanced Raman spectroscopy (SERS). The main approach of this method is placement of the analyzed substance on special substrates, the principle of operation of which is based on the local increase of electromagnetic field near metal nanoparticles (NPs) with plasmonic properties [5–10]. In addition to SERS spectroscopy, metal NPs with plasmonic properties are promising for use in optoelectronics devices, for example, to enhance the luminescence of LEDs [11,12].

The plasmonic properties of metal NPs depend on many factors, such as their material, shape, size, distance between NPs and several others [13]. Based on correlations described in [14,15] and demonstrated in [16–19], it is possible to control the spectral position and intensity of the NPs absorption peak. For example, an increase in the NPs size shifts the absorption peak to the long-wavelength part of the spectra, the absorption intensity increases with

increasing NPs concentration, the width of the absorption peak depends on the dispersion of NPs sizes [16–18].

Various methods are used to obtain metal NPs, for example: the deposition from colloid solutions [12,19,20], the reverse micelle method [16], gas-phase synthesis and ionic implantation [13]. Most of these methods are expensive and technologically complicated, especially for creation of multi-layer nanostructures, and often do not provide uniform NPs arrays, while sol-gel method is devoid of these disadvantages. In addition, chemical synthesis method, such as sol-gel, represents a simple technological process that is carried out without the use of high vacuum and temperatures, and does not require expensive supplies.

This work is devoted to the creation of a simple version of SERS substrates containing high-density uniform arrays of silver (Ag NPs) and gold (Au NPs) nanoparticles obtained from solutions and deposited on substrates of dielectrics or wide-bandgap semiconductors to replace commercial substrates with cheaper analogs produced in the laboratory. The sol-gel method allows easy modification of the material, size and shape of NPs, which determine their plasmonic properties, and provides wide

---

\* Corresponding author: P.A. Bogdanov, e-mail: [pashabogdanov99@mail.ru](mailto:pashabogdanov99@mail.ru)

opportunities for the selection of SERS substrates for specific tasks and objects under study.

## 2. MATERIALS AND METHODS

To obtain Ag and Au NPs, separate solutions based on silver nitrate ( $\text{AgNO}_3$ ) and chloroauric acid ( $\text{HAuCl}_4$ ), respectively, were prepared in 2-methoxyethanol. The solutions concentrations used were 0.03 and 0.06 M for different samples series. Next, the solutions were mixed on a magnetic stirrer for 5 minutes and were immediately coated to the substrate.

The NPs solutions were coated on quartz substrates by spin-coating method at a speed of 2500 rpm for 15 seconds, the process was repeated 5 times with intermediate drying at 300 °C for 3 minutes. After that, the obtained NPs layers were annealed in a muffle furnace at a temperature of 500 °C for 15 minutes.

Besides pure quartz substrates, NPs layers were also coated on buffer layer of zinc oxide (ZnO). ZnO was chosen as a material of buffer layer based on several points. Firstly, the technology of obtaining ZnO by the sol-gel method is well studied and simple, and a sol composition based on 2-methoxyethanol has been previously developed, which allows to obtain polycrystalline zinc oxide films with high uniformity and smooth surface [21,22]. Secondly, the coating of different material layers from sols based on a single solvent allows for better adhesion and the quality of interlayer boundaries [23]. Thirdly, ZnO has a high optical transmittance in the visible range, which comply not only with the requirements for SERS substrates, but also allow for the study of the optical properties of the NPs arrays themselves.

The ZnO layers were also made by sol-gel method. The ZnO solution was made by dissolving zinc acetate (ZnAc) in 2-methoxyethanol with a concentration of 0.2 M. Monoethanolamine (MEA) was used as a surfactant, the molar ratio of MEA/ZnAc was 1:1. The solution

was stirred for 1 hour to complete dissolution of ZnAc. Deposition of ZnO was carried out in accordance with the method described above for obtaining of NPs. In general, the method of obtaining Ag NPs and ZnO layer has been described in detail in our previous works [21,22].

Mixing the solutions with  $\text{AgNO}_3$  and  $\text{HAuCl}_4$  led to immediate sediment deposition, that made it impossible to obtain a uniform layer on the substrate surface by spin-coating method. Therefore, to obtain mixed Ag and Au NPs array, alternate coating of Ag and Au NPs solutions was carried out layer by layer and in equal proportion on quartz substrates with a ZnO buffer layer. Thus, 5 layers of zinc oxide, 5 layers of a solution of Ag NPs and 5 layers of a solution of Au NPs were coated to the substrates sequentially. After that the obtained samples were annealed in a muffle furnace at 500 °C for 15 minutes.

NPs array morphology and NPs sizes were studied by scanning electron microscopy (SEM) using Mira 3 (Tescan, Czech Republic) and Digital Micrograph software (USA).

The study of the optical properties of the samples was carried out using fiber optic spectrometer AvaSpec 2048 (Avantes, USA), suitable for measuring the samples spectra of absorption, transmittance and optical density in the spectral range of 200–1100 nm.

## 3. RESULTS AND DISCUSSION

The optical absorption spectra of the NPs array obtained on the substrates and on the ZnO buffer layers was measured. The spectra of samples with arrays of Au NPs contained absorption peak in the range of 540–570 nm (Fig. 1), corresponding to the plasmon resonance in Au NPs [17,18]. It can be seen from the spectra that the use of zinc oxide buffer layer led to a small shift of the absorption peak from 565 nm to 545 nm, and to double increase in the absorption peak of Au NPs compared to the sample without a buffer layer.

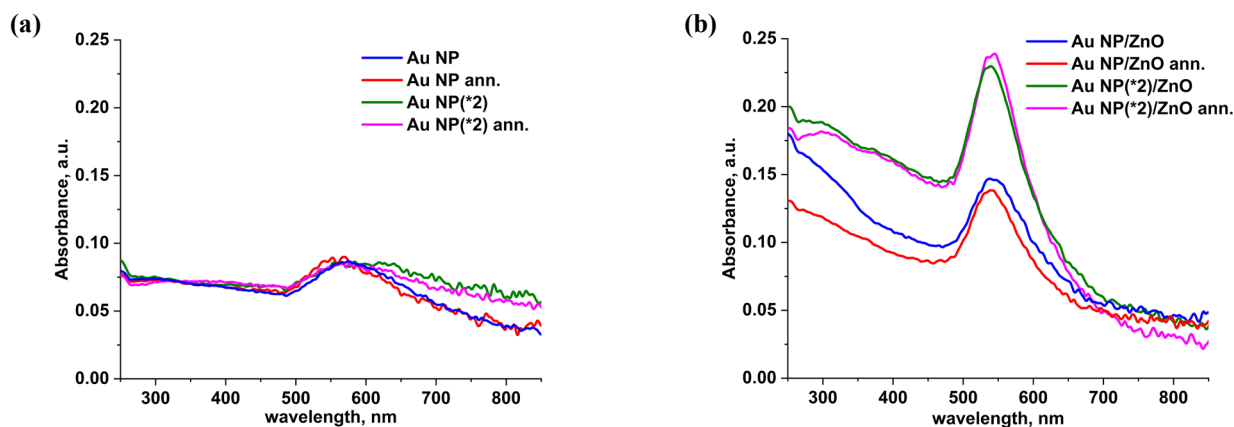


Fig. 1. Optical absorption spectra of Au NPs before and after annealing: (a) without and (b) with ZnO buffer layer.

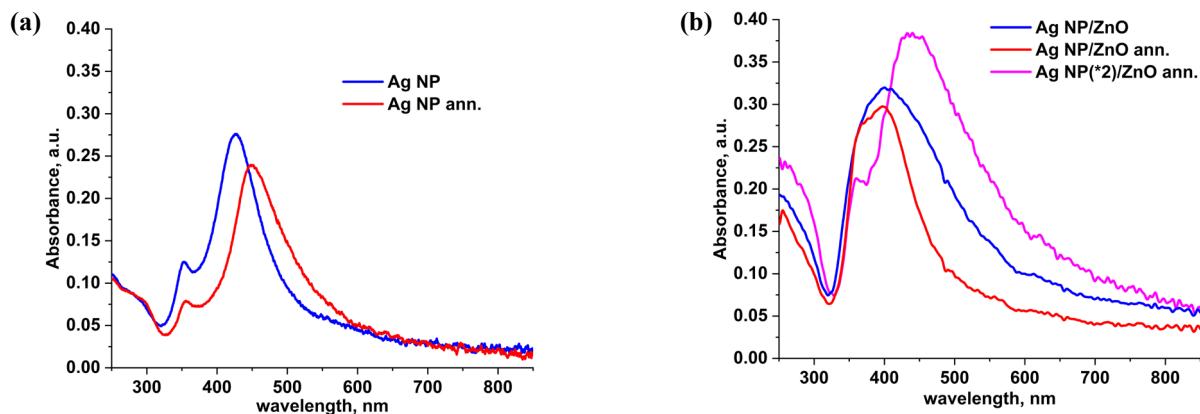


Fig. 2. Optical absorption spectra of Ag NPs before and after annealing: (a) without and (b) with ZnO buffer layer.

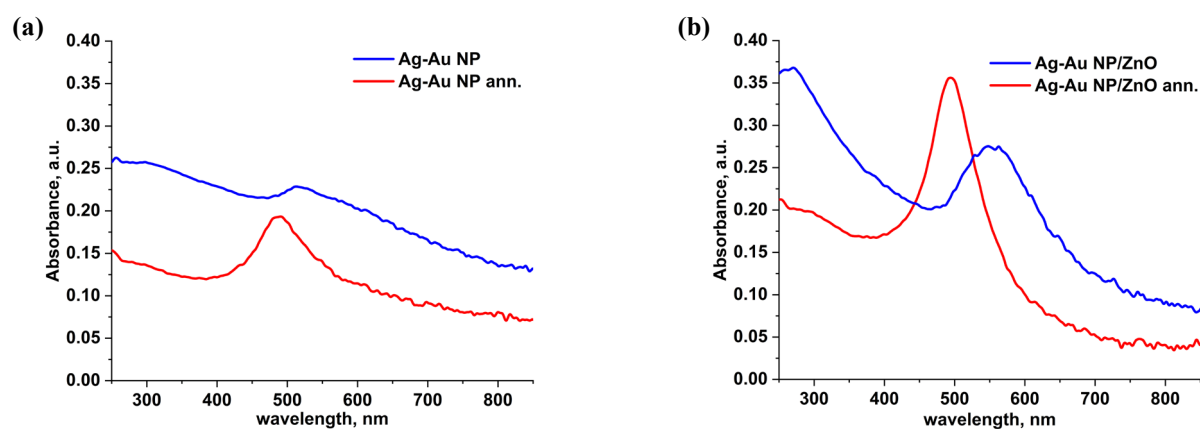


Fig. 3. Optical absorption spectra of mixed Ag and Au NPs arrays: (a) without and (b) with ZnO buffer layer.

It was found that with a doubling of the  $\text{HAuCl}_4$  solutions concentration, the absorption peak of Au NPs without the buffer layer does not change, while in presence of ZnO buffer layer the intensity is doubled. An annealing of samples with Au NPs with and without a zinc oxide buffer layer did not significantly influence the absorption spectra.

The spectra of samples with arrays of Ag NPs contained absorption peak in the range of 400–450 nm (Fig. 2), corresponding to the plasmon resonance in Ag NPs [16,17]. It can be seen from the spectra that the use of a zinc oxide buffer layer led to an increase in intensity and a shift of the Ag NPs plasmon peak to shorter wavelengths in comparison with the sample without a buffer layer. Doubling the concentration of  $\text{AgNO}_3$  solutions led to the increase in the Ag NPs absorption peak intensity by more than 20%, and to the shift of the absorption peak from 400 nm to 440 nm. Annealing of samples with Ag NPs, as well as with Au NPs, with and without a zinc oxide buffer layer did not significantly affect the absorption spectra.

The optical absorption spectra of the obtained samples with mixed Ag and Au NPs array also contained absorption peak in the range of 490–560 nm, corresponding to the plasmon resonance in Ag and Au NPs (Fig. 3). It

should be noted that the Ag and Au NPs coating sequence did not influence the optical properties of total arrays of Ag and Au NPs. A comparison of the spectra in Fig. 3 shows that, as in the case of only Au NPs, the use of the ZnO buffer layer increases the intensity of the absorption peak of mixed arrays of Ag and Au NPs. When comparing the absorption spectra before and after annealing (Fig. 3), it was found that the mixed Ag and Au NPs arrays as a result of annealing is characterized by a decrease and broadening of the NPs absorption peak, and also by the shift of the absorption peak from 510 nm to 490 nm for NPs without the ZnO buffer layer and from 560 nm to 495 nm with it.

An increase in the NPs absorption intensity while maintaining the wavelength is most often associated with an increase in the density of the NPs array, and a shift in the wavelength of the plasmon peak is observed when their size or shape changes [13–15]. Probably, for NPs arrays obtained in this work the presence of a buffer layer of zinc oxide led to an improvement in sol adhesion to the substrate during spin-coating.

It was previously shown [21] that an array of Ag NPs is formed as a result of the silver diffusion over the

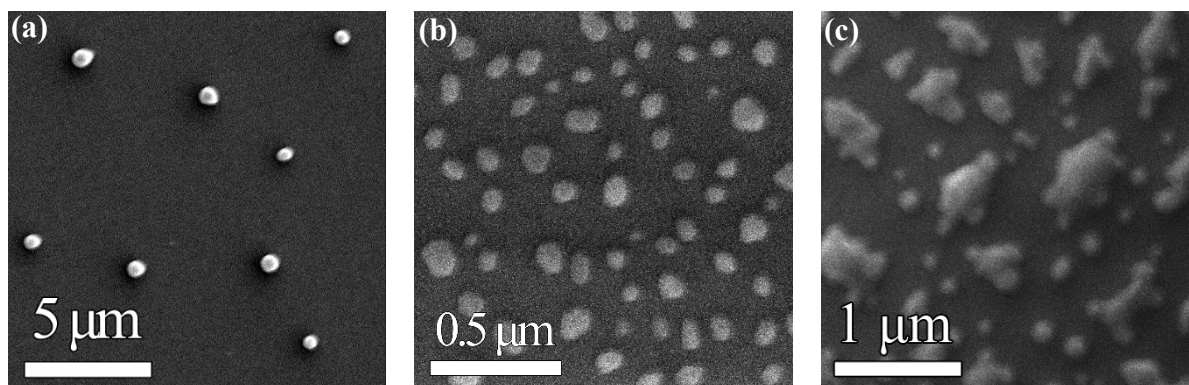


Fig. 4. SEM images of the surface of obtained NPs arrays: (a) Ag NPs, (b) Au NPs, (c) mixed Ag and Au NPs arrays.

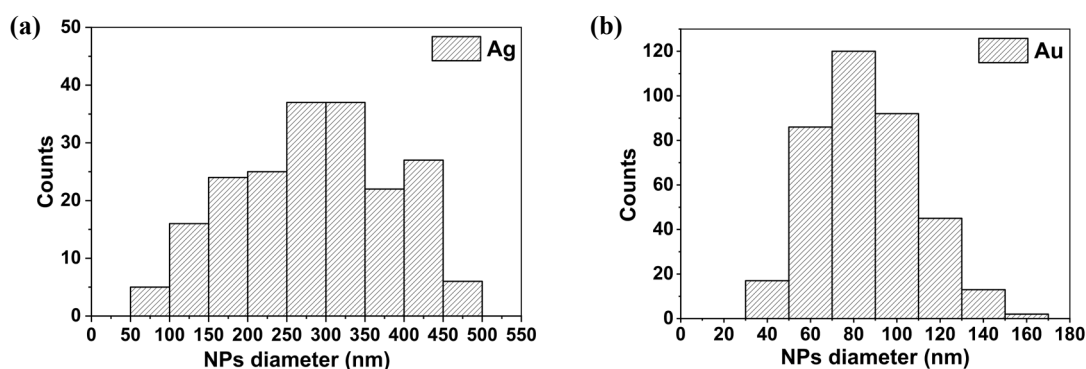


Fig. 5. NPs size distribution histograms constructed from SEM data: (a) Ag NPs, (b) Au NPs.

substrate surface during annealing. Probably, the presence of a zinc oxide buffer layer affects the diffusion efficiency, which leads to a change in the size and density of the obtained NPs. In addition, the zinc oxide buffer layer, due to its polycrystalline structure and structured surface, changes the distribution of the NPs material over the substrate surface, which leads to a change in the parameters of the obtained NPs array. In the case of bigger Ag NPs, the diffusion processes undergo greater changes than for smaller Au NPs. Fig. 4 shows the results of the SEM study of the obtained NPs array. Based on the SEM images NPs size distribution histograms were constructed (Fig. 5). Au NPs have sizes from 50 to 110 nm, Ag NPs are larger and reach sizes of 200–400 nm. The NPs sizes in the mixed Ag and Au array correspond to the sizes in the separate NPs layers.

The SEM images of the obtained NPs (Fig. 4) do not demonstrate ordering in arrays. However, the NPs arrays show the uniformity, i.e., their surface density remains approximately at the same level throughout the substrate. NPs in the separate arrays are uniformly distributed over the substrate surface without agglomeration and clustering. The NPs density was determined using SEM images and was equal to the number of NPs in a unit area of the substrate surface. The surface density of NPs was  $3.3 \cdot 10^9 \text{ cm}^{-2}$  in the sample with Au NPs and  $3.1 \cdot 10^6 \text{ cm}^{-2}$

in the sample with Ag NPs. But in the sample with mixed array of Ag and Au NPs the surface density was lower than their sum –  $5.7 \cdot 10^8 \text{ cm}^{-2}$ . Probably, as observed in the SEM image, large Ag NPs agglomerate on themselves several small Au NPs, so the total surface density of the NPs array is slightly lower (Fig. 4).

#### 4. CONCLUSION

The uniform arrays of Ag and Au NPs with surface density up to  $3.3 \cdot 10^9 \text{ cm}^{-2}$  were made by sol-gel method. To obtain NPs with various plasmonic properties, the concentration of solutions, the modes of their synthesis and layer coating were varied. The absorption spectra of obtained samples contained a peak in the visible area corresponding to the plasmonic resonance of the Ag and Au NPs. It was found that the wavelength of plasmon absorption peak of NPs depends on the synthesis modes, therefore, the characteristics of NPs arrays can be controlled by conditions of synthesis. The use of ZnO buffer layers for coating of NPs leads to an increase in the intensity of the NPs plasmon peak compared to samples without the ZnO buffer. The process of annealing leads to a gradual decrease and broadening of the absorption peak of Ag and mixed Ag and Au NPs arrays. But annealing does not affect absorption spectra of Au NPs arrays.

## ACKNOWLEDGEMENTS

The work was supported by the Ministry of Science and Higher Education of the Russian Federation (Project 5082.2022.4).

## REFERENCES

- [1] I. Nabiev, I. Chourpa, M. Manfait. *Applications of Raman and surface-enhanced Raman scattering spectroscopy in medicine*, Journal of Raman Spectroscopy, 1994, vol. 25, no. 1, pp. 13–23.
- [2] L. Fabris, *SERS tags: the next promising tool for personalized cancer detection*, ChemNanoMat, 2016, vol. 2, no. 4, pp. 249–258.
- [3] N. Nuntawong, P. Eiamchai, S. Limwichean, M. Horprathum, V. Patthanasettakul, P. Chindaudom, *Applications of surface-enhanced Raman scattering (SERS) substrate*, 2015 Asian Conference on Defence Technology (ACDT), 2015, pp. 92–96.
- [4] K.C. Doty, C.K. Muro, J. Bueno, L. Halámková, I.K. Lednev, *What can Raman spectroscopy do for criminalistics?*, Journal of Raman Spectroscopy, 2016, vol. 47, no. 1, pp. 39–50.
- [5] M.A. Cauqui, J.M. Rodriguez-Izquierdo, *Application of the sol-gel methods to catalyst preparation*, Journal of Non-Crystalline Solids, 1992, vol. 147, pp. 724–738.
- [6] B. Sharma, R.R. Frontiera, A.I. Henry, E. Ringe, R.P. Van Duyne, *SERS: Materials, applications, and the future*, Materials Today, 2012, vol. 15, no. 1–2, pp. 16–25.
- [7] D. Cialla, A. März, R. Böhme, F. Theil, K. Weber, M. Schmitt, J. Popp, *Surface-enhanced Raman spectroscopy (SERS): progress and trends*, Analytical and Bioanalytical Chemistry, 2012, no. 403, pp. 27–54.
- [8] L.A. Lane, X. Qian, Sh. Nie, *SERS nanoparticles in medicine: from label-free detection to spectroscopic tagging*, Chemical Reviews, 2015, vol. 115, no. 19, pp. 10489–10529.
- [9] A.S.D.S. Indrasekara, S. Meyers, S. Shubeita, L.C. Feldman, T. Gustafsson, L. Fabris, *Gold nanostar substrates for SERS-based chemical sensing in the femtomolar regime*, Nanoscale, 2014, vol. 6, no. 15, pp. 8891–8899.
- [10] S. Lucht, T. Murphy, H. Schmidt, H.-D. Kronfeldt, *Optimized recipe for sol-gel-based SERS substrates*, Journal of Raman Spectroscopy, 2000, vol. 11, no. 31, pp. 1017–1022.
- [11] D.V. Guzatov, S.V. Gaponenko, H.V. Demir, *Possible plasmonic acceleration of LED modulation for Li-Fi applications*, Plasmonics, 2018, vol. 13, no. 6, pp. 2133–2140.
- [12] R.R. Shamilov, V.I. Nuzhdin, V.F. Valeev, Yu.G. Galyametdinov, A.L. Stepanov, *Enhancement of Photoluminescence of the CdSe/CdS Quantum Dots on Quartz Substrates in the Presence of Silver Nanoparticles*, Technical Physics, 2016, vol. 61, no. 11, pp. 1698–1703.
- [13] V.V. Klimov, *Nanoplasmonics*, Fizmatlit, Moskva, 2010 (in Russian).
- [14] E. Petryayeva, U.J. Krull, *Localized surface plasmon resonance: Nanostructures, bioassays and biosensing-A review*, Analytica Chimica Acta, 2011, vol. 706, no. 1, pp. 8–24.
- [15] P. Han, W. Martens, E.R. Waclawik, S. Sarina, H. Zhu, *Metal Nanoparticle Photocatalysts: Synthesis, Characterization, and Application*, Particle & Particle Systems Characterization, 2018, vol. 35, no. 6, art. no. 1700489.
- [16] S.I. Rasmagin, L.A. Apresyan, *Analysis of the optical properties of silver nanoparticles*, Optics and Spectroscopy, 2020, vol. 128, pp. 327–330.
- [17] V.I. Shevtsova, P.I. Gaiyduk, *Spectral position of the surface plasmon resonance line of silver and gold nanoparticles colloidal solutions*, Vestnik BSU, 2012, vol. 1, no. 2, pp. 15–18 (in Russian).
- [18] Y. Kobayashi, M.A. Correa-Duarte, L.M. Liz-Marzán, *Sol-gel processing of silica-coated gold nanoparticles*, Langmuir, 2001, vol. 17, no. 20, pp. 6375–6379.
- [19] M. Zhang, X. Cao, H. Li, F. Guan, J. Guo, F. Shen, Y. Luo, C. Sun, L. Zhang, *Sensitive fluorescent detection of melamine in raw milk based on the inner filter effect of Au nanoparticles on the fluorescence of CdTe quantum dots*, Food Chemistry, 2012, vol. 3, no. 135, pp. 1894–1900.
- [20] B. Sharma, M.F. Cardinal, S.L. Kleinman, N.G. Greeneltch, R.R. Frontiera, M.G. Blaber, G.C. Schatz, R.P. Van Duyne, *High-performance SERS substrates: Advances and challenges*, MRS Bulletin, 2013, vol. 8, no. 38, pp. 615–624.
- [21] L.A. Sokura, E.A. Ryabkova, D.A. Kirilenko, E.V. Shirshneva-Vaschenko, *Structural and Optical Properties of Silver Nanoparticles In Situ Synthesized in ZnO Film by Sol-Gel Method*, Rev. Adv. Mater. Technol., 2021, vol. 3, no. 4, pp. 29–33.
- [22] L.A. Sokura, E.V. Shirshneva-Vaschenko, D.A. Kirilenko, Zh.G. Snezhnaia, P.S. Shirshnev, A.E. Romanov, *Electron-microscopy study of ordered silver nanoparticles synthesized in a ZnO:Al polycrystalline film*, Journal of Physics: Conference Series, 2019, vol. 1410, art. no. 012170.
- [23] E.V. Shirshneva-Vaschenko, L.A. Sokura, P.S. Shirshnev, D.A. Kirilenko, Zh.G. Snezhnaia, D.A. Bauman, V.E. Bougrov, A.E. Romanov, *Preparation of transparent n-ZnO:Al/p-CuAlCrO<sub>2</sub> heterojunction diode by sol-gel technology*, Rev. Adv. Mater. Sci., 2018, vol. 57, pp. 167–174.

УДК 535.34

## Синтез однородных массивов наночастиц Ag и Au методом ЗОЛЬ-ГЕЛЬ

П.А. Богданов<sup>1</sup>, Л.А. Сокура<sup>1,2</sup>, А.В. Кремлева<sup>1</sup>, В.В. Виткин<sup>1</sup>

<sup>1</sup> Институт перспективных систем передачи данных Университета ИТМО, Кронверкский пр., д. 49, лит А, Санкт-Петербург, 197101, Россия

<sup>2</sup> ФТИ им. Иоффе РАН, ул. Политехническая, д. 26, Санкт-Петербург, 194021, Россия

**Аннотация.** Методом золь-гель на поверхности буферных слоев оксида цинка получены однородные массивы наночастиц серебра и золота плотностью более  $3,3 \cdot 10^9 \text{ см}^{-2}$ . Проводилось варьирование состава, концентрации и режимов синтеза растворов, нанесения и последующей термообработки слоев. Полученные образцы в спектре поглощения содержали пик в видимой области, соответствующий плазмонному резонансу в наночастицах Ag и Au. Обнаружено, что длина волны и интенсивность пика плазмонного поглощения наночастиц меняется в зависимости от условий их синтеза. Например, использование буферных слоев ZnO приводит к увеличению интенсивности плазмонного пика наночастиц Ag и Au. Отжиг приводит к постепенному уменьшению интенсивности и уширению пика поглощения наночастиц Ag и смешанных массивов наночастиц Ag и Au, но интенсивность и длина волны пика плазмонного поглощения наночастиц Au при отжиге не изменяется.

**Ключевые слова:** SERS; золь-гель синтез наночастиц; пик плазмонного поглощения; наночастицы серебра и золота; растровая электронная микроскопия